Engineering Structures 289 (2023) 116305

Contents lists available at ScienceDirect

Engineering Structures

journal homepage: www.elsevier.com/locate/engstruct

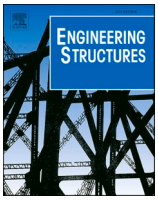

Feasibility of structural retrofit concrete pipelines using limestone calcined clay cement Engineered Cementitious Composites (LC3 ECC)

He Zhu [a], Tianyu Wang [a], Yichao Wang [a,b], Wei-Hsiu Hu [a], Victor C. Li [a,*]

[a] Department of Civil and Environmental Engineering, University of Michigan, Ann Arbor, MI 48109, USA
[b] School of Civil Engineering, Shijiazhuang Tiedao University, Shijiazhuang, Hebei Province 050043, China

ARTICLE INFO

Keywords:
Engineered Cementitious Composites (ECC)
Pipe
Retrofit
Leak-proof
Permeability

ABSTRACT

Advances in pipeline rehabilitation technology are urgently needed to address aging concrete pipelines operating in aggressive conditions. Current repair methods have limitations on enhancing pipe structurally. In this research, ductile ECC was employed as a durable retrofitting material for concrete pipe. Firstly, two strength grades of ECC were developed. Tensile strain capacity ranging from 5.4 to 9.3 % was obtained. Owing to the tailored crack width (average 61.6 μm at 8% strain) and self-healing capacity, the 2% pre-tensioned ECC retained 10^{-10} m/s of the coefficient of permeability after 14 d of testing. The cracked concrete pipe was repaired by ECC/mortar, then examined by three-edge loading and flexural tests. Although ECC had lower strength than the referenced mortar, ECC-repaired pipe attained higher load and deformation capacity than the mortar-repaired pipe. ECC distributed the macro crack into multiple tiny cracks, leading to the pipe being an oval shape with residual load capacity after crushing, compared to the brittle failure of the mortar-repaired pipe. The cracked ECC pipe retained its structural integrity and enabled the intrinsic leak-proof function of the cracked ECC pipe. Finally, ECC demonstrated the ability to structurally and functionally (leak-proof) retrofit the concrete pipe, suggesting a durable promising repair material for concrete pipe.

1. Introduction

In the context of fast urbanization, cities are experiencing increased population and activities, with increasing burden on the drinking water and wastewater system. Concrete is the predominant material for water pipes, making up more than 50% of water pipe systems [1]. Concrete has limited tensile capacity, so it is prone to cracking under loads, including water pressure, traffic load, poor bedding, temperature, and shrinkage. In addition, many aging concrete pipes are in deteriorated status due to the aggressive working conditions [2]. Failures such as pipe bursting, sewage spills, and traffic interruptions have been widely documented [1]. In the US, more than 5.5 million km of water pipelines have been installed. There is a water main break every two minutes and an average of 1–4.8% of pipelines are to be replaced or repaired [3]. Aging pipes as well as the aggressive working conditions lead to tremendous opportunities for pipeline rehabilitation.

Current pipe rehabilitation technologies have limitations, especially on structural retrofit. Cure-in-place-pipe (CIPP) is the most popular method for trenchless pipeline repair. A lining tube immersed with resin is installed in a host pipe. The liner is then hardened by heat/ultraviolet curing [4]. Although CIPP can attain a strengthening effect under internal pressure, limited enhancement for resisting external loading can be established due to the low stiffness of the CIPP liner [5]. Moreover, the high cost and environmental concerns remain challenging [6]. Close-fit method folds or reduces the diameter of a new pipe before insertion, and reverts the new pipe diameter after installation so that the new pipe liner fits snugly with the host pipe [7]. Similar to CIPP, the close-fit pipe attained limited structure ability under external loading. Internal or external grouting method has been proven effective to repair local leakage or fill voids [8]. Although the leakage function can be restored after grouting, less structural strengthening is obtained.

Some pipe structural enhancement technologies have been attempted. However, these methodologies suffer from trade-offs. For example, sliplining pushes or pulls a new smaller pipe into the original concrete pipe and grouts the annular space to form a new composited pipe (old pipe-grout-new pipe) [9]. By the combined effect of grout and the new pipe liner, the damaged pipe can be structurally strengthened under both external and internal loads. Nevertheless, the section area of the

* Corresponding author.
E-mail addresses: zhuhe@umich.edu (H. Zhu), tianyuwang@ust.hk (T. Wang), wangyichao@stdu.edu.cn (Y. Wang), hwhsiu@umich.edu (W.-H. Hu), vcli@umich.edu (V.C. Li).

https://doi.org/10.1016/j.engstruct.2023.116305

Available online 14 May 2023

pipeline was significantly reduced. Spray-in-place pipe with high-performance concrete/mortar, geopolymer, or polymetric materials can enhance the load capacity after repair, which also required a relatively large liner thickness, resulting in the flow capacity the same as the sliplining method [10,11]. The compromised hydraulic capacity caused by the increased liner thickness does not meet the increased demand to support dense urbanization. Moreover, due to the brittle nature of concrete/mortar/geopolymer, once the crack is initiated in the concrete/mortar/geopolymer liner, it will propagate suddenly across the liner and the repaired pipe, resulting in the failure of rehabilitation.

Engineered Cementitious Composites (ECC) suggest a potential solution of thinner liner thickness and ductile failure mode, and hold promise as a durable strengthening material for concrete pipes rehabilitation [1,12]. ECC is a specific fiber-reinforced concrete with the deliberate design of matrix, fiber, and fiber–matrix interface. Distinct from conventional fiber-reinforced concretes, ECC exhibits a tensile strain-hardening behavior, ultra-high tensile ductility (usually greater than 3% of tensile strain capacity), and controlled crack width (e.g. below 100 μm) [13]. Moreover, the unhydrated cement grains of ECC combined with the tiny crack width endows ECC with an intrinsic self-healing ability [14,15]. The healed cracks significantly reduce the permeability of the cracked ECC [16], suggesting that the ECC liner can mitigate the leakage even under cracking conditions. The robust self-healing ability of ECC has been demonstrated in different curing environments, including water, water–air cycle, salt, acid, and alkaline conditions [17–20], which indicates ECC is a durable material in pipe applications.

As guided by the micro-mechanical design theory [13], ECC does not include coarse aggregates. This result in high cement content, which increases environmental concerns as cement is a carbon-intensive ingredient [21]. A high volume of supplementary cementitious materials (SCMs) has been used to mitigate the high carbon footprint of ECC. The SCMs used include fly ash, slags, silica fume, iron ore tailings, limestone, calcined clay, rice husk ash, and recycled fine powder [13,14,22–27]. Among the adopted SCMs, limestone calcined clay cement (LC3) has attracted increasing interest in the concrete industry as a low-carbon blended cement due to its abundant availability [28]. LC3 has established satisfactory mechanical [14,29,30] and rheological [12,31–33] performance at the material level. More investigations are needed to utilize LC3 ECC in retrofitting/repairing concrete pipes with satisfied structural performance and greenness advantages.

Although ECC has been applied in structural retrofits, such as dams, irrigation channels, and masonry [1,13,34,35], its application in pipeline retrofit is rarely studied. Authors have developed centrifugally sprayed ECC for pipe repair, and structural enhancement under a three-edge bearing load was demonstrated by ECC with a reduced thickness [12,32,33]. More studies on the performance of ECC retrofitted pipe, including the effect of bending load on permeability, are needed.

This study aims at establishing ECC as a sound retrofitting material for concrete pipe rehabilitation at a lab scale, providing guidance for future field applications and designs. Specifically, two strength grades of ECC were developed. Their uniaxial tensile performance and water permeability, were examined at the material level. Finally, the ECC was applied to repair cracked concrete pipes. Three-edge bearing capacity and bending capacity were tested to demonstrate the retrofit effect of ECC. A leak-proof function of the repaired pipe was experimentally verified.

2. Experimental program

2.1. Materials design and preparations

Table 1 lists the chemical compositions of the binders, including ordinary Portland cement (OPC), metakaolin (MK), limestone (LS), fly ash (FA), and silica fume (SF). Herein, LC3 was blended by OPC, MK, and LS at the ratio of 55:30:15 [14,31]. F-75 grade silica sand was utilized as fine aggregates. To induce the multiple cracks of LC3 ECC, crumb rubber (CR) powders (with an average particle size of 275 μm) were adopted to replace part of the sand. Fig. 1 shows the particle size distribution of dry materials.

To demonstrate the advantages of the ECC liner, two strength grades of LC3 ECC were developed, meanwhile, mortars with compressive strength of 45.1 MPa (M40) and 68.6 MPa (M70) were designed as reference compositions. Table 2 lists the mixed compositions of ECC and mortars. E20-CR0 is a low-strength ECC (20 MPa grade compressive strength) with no CR. Polypropylene (PP) fibers were used in E20-CR0 to develop the low-cost ECC, while polyethylene (PE) fibers were adopted in E40-CR0 for developing a higher strength ECC (40 MPa grade). Table 3 summarizes the parameters of PE and PP fibers. 30 kg/m^3 and 50 kg/m^3 of CR were added in E40-CR30 and E40-CR50 to tailor the crack width, respectively. The mortar Pipe_Ref was utilized for casting the original pipe. M40 and M70 were two mortar mixes for repaired liners.

A water reducer (WR) was utilized for tailoring the fresh properties suitable for fiber dispersion. A mini-slump cone (diameter = 10 cm) per ASTM C1437 [36] was used for the flow table test. After lifting the mini-cone, the mortars (Pipe_Ref, M40, and M70) spread on the flow table, and the spread diameter was measured once the pastes come to a rest. Due to the addition of fiber, ECC tends to retain its shape under self-weight, so the flow table was dropped 25 times in 15 s per ASTM C1437 [36]. The spread diameter of ECCs and mortars were listed in Table 2,

The dry ingredients (OPC, MK, LS, FA, SF, silica sand, and CR if used)

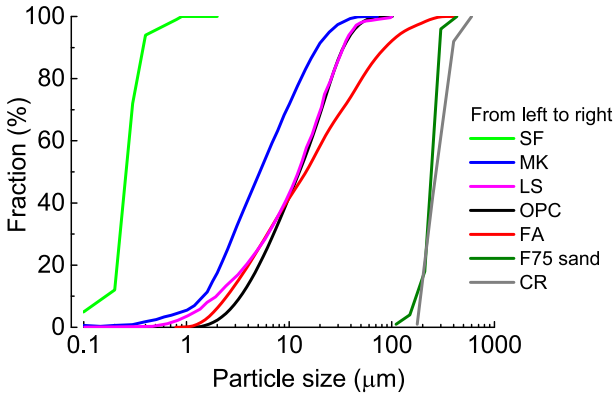

Fig. 1. Particle size distributions of dry ingredients.

Table 1
Chemical compositions of binder ingredients (mass %).

Ingredients	CaO	Al_2O_3	SiO_2	Fe_2O_3	MgO	SO_3	K_2O	TiO_2
OPC	63.5	4.8	19.6	2.9	2.2	2.6	0.6	0.3
MK	0.0	46.6	50.8	0.5	0.0	0.1	0.3	1.6
LS	55.3	0.0	0.0	0.0	0.0	0.0	0.0	0.0
FA	17.5	21.8	39.4	11.5	3.7	1.9	1.1	1.2
SF	0.4	0.7	96.5	0.3	0.5	0.5	0.85	0.0

Note: LS is a highly pure $CaCO_3$ powder, and the main composition is CaO.

Table 2
Mixture design of ECC and mortars (unit: kg/m^3).

Mixture	OPC	MK	LS	FA	SF	CR	F75	W	WR	PE	PP	Spread diameter (mm)
E20-CR0	270	147	73	1077	0	0	0	470	2	0	20	185
E40-CR0	330	180	90	720	0	0	404	330	8	20	0	183
E40-CR30	330	180	90	720	0	30	404	330	8	20	0	185
E40-CR50	330	180	90	720	0	50	404	330	8	20	0	182
Pipe_Ref	500	0	0	0	0	0	1200	200	6	0	0	240
M40	330	180	90	720	0	0	404	330	6	0	0	220
M70	500	0	0	0	75	0	1200	150	16	0	0	213

Table 3
Technical parameters of PP and PE fibers.

Fiber type	Diameter (μm)	Length (mm)	Nominal strength (GPa)	Young's Modulus (GPa)	Rupture elongation (%)	Density (g/cm^3)
PP	12	10	0.85	6	21	0.91
PE	24	12	2.90	100	2.4	0.97

were pre-mixed for 5 min using a Hobart planetary mixer at first speed (94 rpm). Water premixed with the water reducer was added and further mixed for 5 min at 94 rpm to obtain the uniform paste. For Pipe_Ref, M40, and M70, the prepared paste was ready for casting concrete pipe or mortar liners. For the ECC mixes, fibers were added to the fresh pastes and mixed at a second speed (174 rpm) for an additional 5 min.

2.2. ECC samples and tests

Air curing facilitates the multiple-cracking of ECC, while water curing enhances the matrix strength and may lead to a decreased ductility [12,13], therefore, ECC samples were cured in air (20 ± 3 ℃, 40 ± 5% RH) for 28 d before tests. 50-mm cube samples were adopted for the compressive strength test. Dogbone samples (Fig. 2) were performed on an Instron machine conducting uniaxial tensile tests at 1 mm/min [12]. The deformation was measured by averaging the reading of two linear variable displacement transducers (LVDT). The gauge length (around 80 mm) was shown as the green part in Fig. 2. Average crack width was calculated by dividing the displacement by the crack number within the gauge length. The results were obtained by the average value of three specimens.

The dogbone specimens of E20-CR0, E40-CR0, and E40-CR30 were pre-tensioned to 1% and 2% strain levels at 28 d. Then the cracked specimens were placed horizontally in a falling head setup (Fig. 3) to

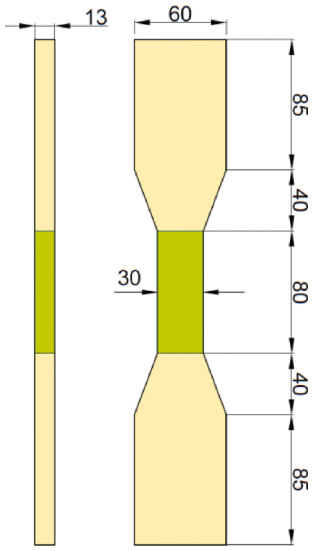

Fig. 2. Dogbone-shaped specimen for uniaxial tension test (unit: mm).

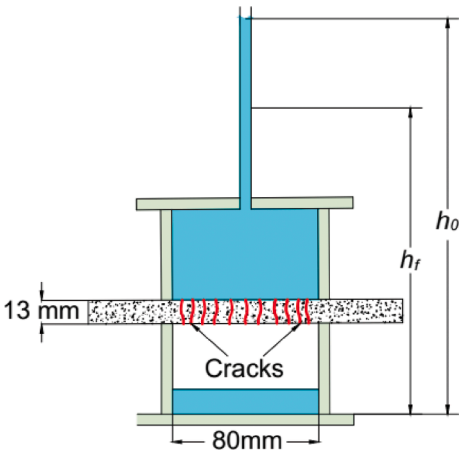

Fig. 3. Permeability test.

measure the permeability of ECC under a hydraulic gradient suggested by Lepech and Li [16]. The edges of the specimen were sealed with silicone sealant. Due to the long period of permeability tests, the pre-cracked specimens were conducted in an unloaded state. Monitoring of the coefficient of permeability (*CoP*) started 2 h after the specimens' seal and lasted 14 d, i.e. from the age of 28 d to 42 d. Each permeability test included two specimens. The *CoP* was calculated using equation (1).

$$CoP = \frac{a}{A}\frac{b}{t_f}\ln\left(\frac{h_0}{h_f}\right) \quad (1)$$

where the notations' meaning and value are listed in Table 4.

2.3. Pipe fabrication and repair protocol

Pipe_Ref was used for preparing the concrete pipe, which was formed by two concentric kraft tube molds. The 200 mm diameter and 150 mm

Table 4
Physical meaning of parameters for permeability test.

Notation	Physical meaning	Value
a	the cross-sectional area of the standpipe	2.84×10^{-5} m^2
A	the cross-sectional area subject to flow	1.78×10^{-2} m^2
b	the specimen thickness in the direction of flow	13 mm
t_f	test duration	Measured
h_0	initial hydraulic head	Measured
h_f	final hydraulic head at the time t_f	Measured

diameter tubes were fixed by a cross fixture (Fig. 4(a)) to generate a concrete pipe with 25 mm-wall thickness (Fig. 4(c)). A steel cage made of steel mesh (1.6 mm diameter, 25 mm*50 mm opening size) was placed between the two tubes (12.5 mm cover thickness). After the concrete was poured into the pipe mold, the whole mold was vibrated for 60 s on a vibration table. After curing for 7 days in air, the pipe as well as the kraft mold was immersed in the water so that the wet kraft mold can be peeled off. Fig. 4(b) shows the appearance of the fabricated pipe (900 mm length).

After curing in air for 28 days, 900 mm length pipes were pre-cracked under a four-point bending load (Fig. 5(a)) at a 0.6 mm/min rate. The deflection of the pipe was measured by OPTOTRAK sensors. Once the crack was initiated, the test was stopped. Meanwhile, the unloaded 900 mm-length concrete pipe was cut into 200 mm-length sections, which were used for the three-edge bearing test per ASTM C497 [37]. The 200-mm length pipe sections were pre-cracked at a loading rate of 0.1 mm/s (Fig. 5(b)) [37]. Two samples per batch were tested for crushing and bending tests.

Then the cracked pipe as well as a 110-mm diameter kraft tube was fixed by the cross-fixture (Fig. 4(a)). E20-CR0, E40-CR30, M40, and M70 were poured from the gap between the pipe and kraft tube to form a 20 mm thickness of repaired liner (Fig. 4(d)). With additional 28 days of air curing, the repaired performance of the concrete pipe-repaired liner was again examined by four-point bending (Fig. 5(a)) and three-edge bearing tests (Fig. 5(b)).

3. Experimental results and discussions

3.1. Compressive and tensile results

Table 5 lists the compressive and tensile results of the developed LC3 ECC. The compressive strength of E20-CR0 was 21.5 MPa, meanwhile, E40-CR0 attained a compressive strength of 42.5 MPa. With the addition of 30 and 50 kg/m^3 of crumb rubber, the compressive strength of E40-CR30 and E40-CR50 were diminished to 38.7 MPa and 32.2 MPa, respectively. The compressive strength of ECCs were all lower than that of Pipe_Ref (48.1 MPa). M40 (45.1 MPa) had a comparable and M70 (68.6 MPa) obtained a higher strength than Pipe_Ref.

The developed LC3 ECC all showed tensile strain-hardening characteristics (Fig. 6). Similar to the low compressive strength, E20-CR0 has an ultimate tensile strength of 2.9 MPa, while E40-CR0 attained 7.1 MPa. The tensile strain capacity of E20-CR0 and E40-CR0 were both higher than 5 %. With the addition of CR, the tensile strain capacity was increased to 9.3 % and 8.7 %, while the ultimate tensile strength was reduced to 6.8 MPa and 6.6 MPa for E40-CR30 and E40-CR50, respectively.

CR acts as artificial flaws to initiate more cracks as well as enhance tensile ductility. The average crack number at failure was 39 for E20-CR0 and 31 for E40-CR0. It was notably increased when CR was included, as E40-CR30 had 107 cracks at failure. However, further increasing the CR content to 50 kg/m^3 contributed little to crack numbers. The crack width of E40-CR0 (around 100 μm) was significantly reduced to 35.3–61.6 μm by E40-CR30. The more saturated cracks with a smaller width of E40-CR30 and E40-CR50 can also be observed in Fig. 7. Excessive CR impaired the mechanical properties while improving the crack width insignificantly. Therefore, E40-CR30 rather than E40-CR50 was considered optimal and was selected for the pipe-repaired liner in this study.

3.2. Permeability results

Fig. 8 illustrates the coefficient of permeability (*CoP*) evolution with age, where all ECC showed a decreased trend of *CoP* with time. 2% pre-tensioned samples showed notably higher *CoP* than that of 1% pre-tensioned samples. As expected, the damaged degree of the ECC affects the magnitude of *CoP*. Moreover, the crack width considerably affects the *CoP*. The initial *CoP* of E20-CR0 for the 1% pre-strained level was 289*10^{-10} m/s at 28 d, corresponding to an average crack width of 51.8 μm. The initial *CoP* of E40-CR0 increased to 887*10^{-10} m/s (95.6 μm-crack width at 1%), while E40-CR30 decreased the *CoP* to 150*10^{-10} m/s due to the tiny crack width (35.3 μm at 1%) tailored by CR. Further increased crack width may result in the exponential growth of *CoP*. For example, a reinforced mortar with 240 μm of crack width yields 7270*10^{-10} m/s of *CoP*, while a 300 μm crack has 28700*10^{-10} m/s of *CoP* [16].

Distinct from concretes or mortars, the *CoP* of the cracked ECC decreased with the evolution of time due to the inherent self-healing ability, and tend to be stable after 14 d of testing (Fig. 8). The portlandite (Ca (OH)$_2$) of the hydration product can react with the CO_2 dissolved in the water, the precipitate $CaCO_3$ seals the tiny cracks of ECC [15], leading to the reduction of permeability. After being immersed in water for 14 d, the *CoP* of developed LC3 ECCs was dramatically diminished by two magnitudes. The *CoP* of E20-CR0 at 42 d was 11.8 and 16.7 *10^{-10} m/s for 1% and 2% pre-strained levels, respectively.

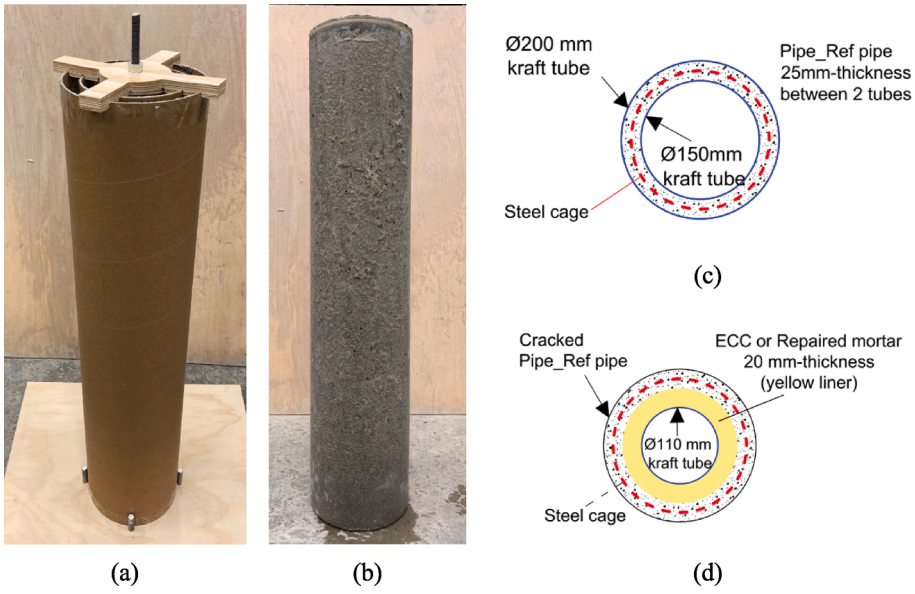

Fig. 4. Pipe fabrication and repair protocol.

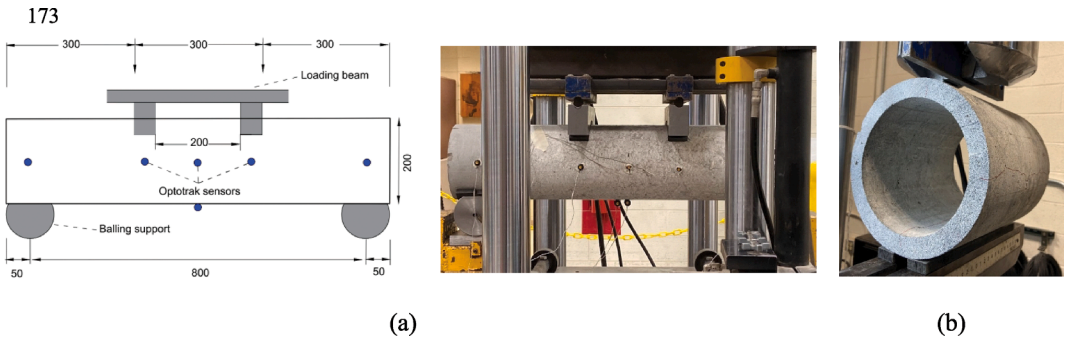

Fig. 5. Pipe loading protocol: (a) four-point bending test and (b) three-edge bearing test (ASTM C497 [37]).

Table 5
Summary of compressive and tensile performance.

Mix ID	f_c/MPa	f_t/MPa	ε_t/%	Crack No.	Average crack width /μm				
					1%	2%	4%	6%	8%
E20-CR0	21.5 ±1.2	2.9 ±0.1	5.4 ±0.6	39 ±6	51.8 ±6.9	61.0 ±7.7	88.5 ±18.2	–	–
E40-CR0	42.5 ±0.3	7.1 ±0.4	5.5 ±1.1	31 ±5	95.6 ±15.6	112.5 ±12.5	126.5 ±12.2	–	–
E40-CR30	38.7 ±0.7	6.8 ±0.3	9.3 ±1.0	107 ±4	35.3 ±1.7	40.3 ±1.9	48.4 ±2.3	48.4 ±2.3	61.6 ±2.9
E40-CR50	32.2 ±2.6	6.6 ±0.4	8.7 ±0.5	102 ±2	36 ±1.3	37.2 ±1.0	45.6 ±1.3	53.3 ±1.6	67.3 ±4.6

*Values means “average value ± standard deviation”.
** Notation meaning: f_c-compressive strength; f_t-ultimate tensile strength; ε_t-tensile strain capacity.
*** The compressive strength of Pipe_Ref, M40, and M70 were 48.1 MPa, 45.1 MP, and 68.6 MPa.

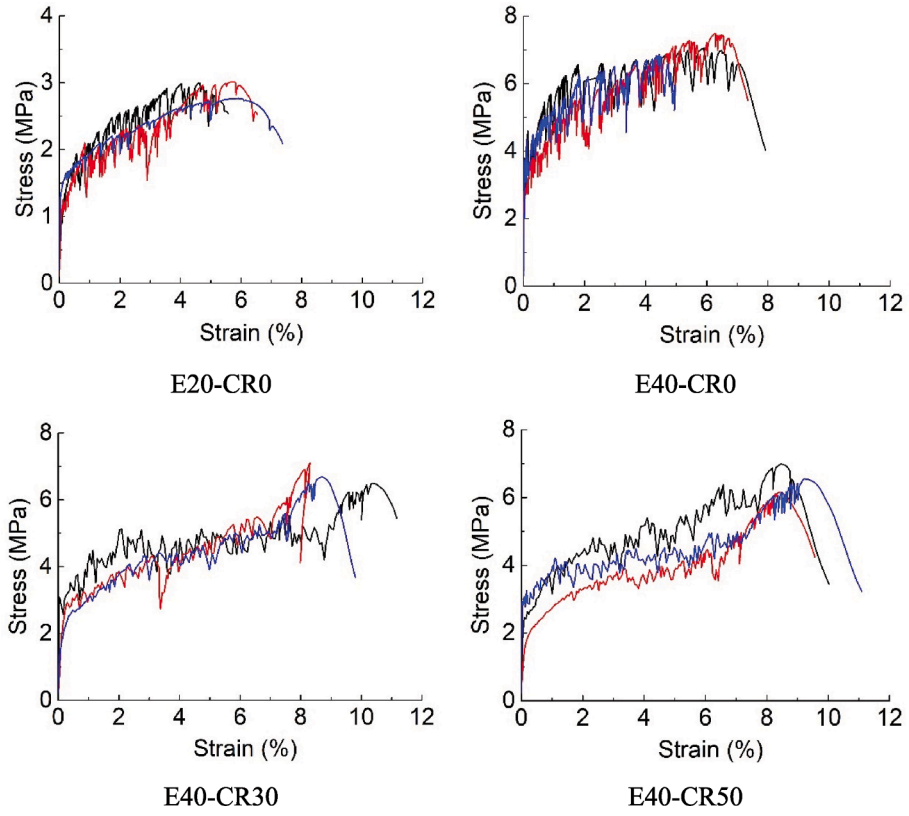

Fig. 6. Stress–strain relationship of developed ECCs.

(a) E20-CR0 (b) E40-CR0 (c) E40-CR30 (d) E40-CR50

Fig. 7. Crack pattern within the 80 mm gauge length of ECCs after tensile failure.

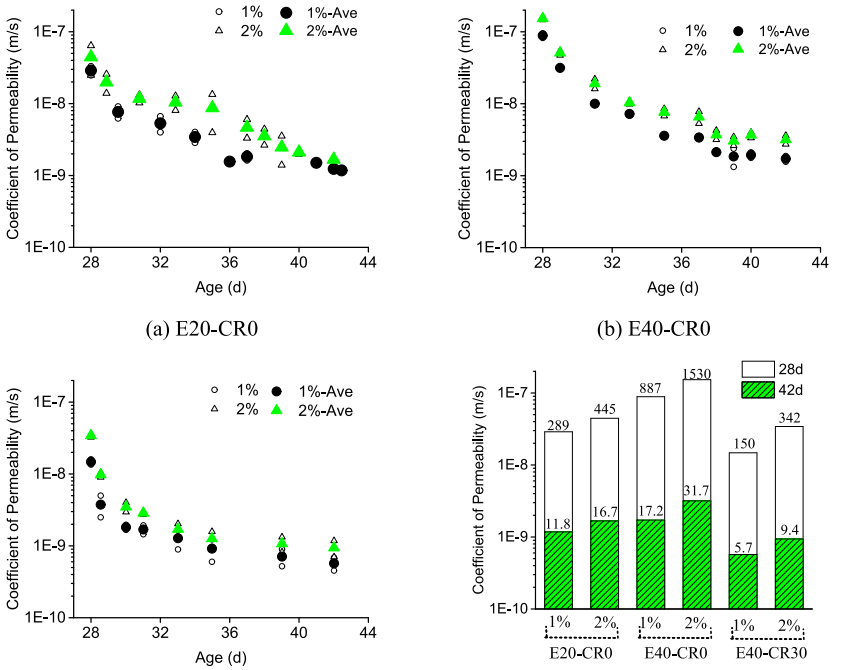

(a) E20-CR0 (b) E40-CR0

(c) E40-CR30 (d) Summary (Column label unit: 10^{-10} m/s)

Fig. 8. The *CoP* evolution from 28d (pre-crack) to 42 d.

Tiny crack width promotes the healing of cracks in ECC, therefore, E40-CR30 attained a *CoP* of 5.77 *10^{-10} m/s at 1% pre-tensioned strain, making up one-third of E40-CR0.

Regarding the permeability test at the concrete pipe level, ASTM497 [37] requires that the concrete pipe present no moist or damp spots on the outer surface after 15 min of water filling, and this time can be extended up to 24 h, corresponding to 10^{-7} m/s of *COP*. The *COP* of uncracked concrete distributes between 10^{-14} and 10^{-10} m/s [38–40], while sound ECC has a comparable *COP* of about 10^{-11} m/s [16]. The previous study [16] shows that *COP* of cracked concrete exceeds 10^{-7} m/s when the crack width is larger than 200 μm. Therefore, cracked concrete pipe usually results in distinct leakage due to its brittleness, in contrast, cracked ECC shows an acceptable *COP* (Fig. 8) according to ASTM497 [37]. Moreover, the ECC liner avoids cracks penetrating along the thickness direction, leading to the water tightness as pipe repaired liner, more details can be found in Section 3.3.

Although LC3 ECC incorporates less OPC compared to the conventional OPC-based ECC [13,41], LC3 ECC retains its self-healing ability [14] and contributes to the reduction of *CoP* with time. Consequently, the developed LC3 ECCs attained comparable *CoP* to OPC-based ECCs

[15,16,42,43], proving that the emerging greener LC3 cement has adequate self-healing potential to seal the cracks.

Water tightness is a critical performance to determine the suitability of ECC for water infrastructures and also represents resistance to the transport of aggressive agents through cracks. The magnitude of both initial and ultimate *CoP* depends on the crack width of the cracked ECC. Via tailoring the crack width, E20-CR0 and E40-CR30 hold promises as a pipe repaired liner material.

3.3. Retrofit performance under three-edge bearing test

The load–displacement results (Fig. 9) show that the pipe repaired with ECC had higher load and displacement capacity than those repaired with mortars. Fig. 10 illustrates the load capacity of intact Pipe_Ref concrete pipe and repaired pipe with different materials. Surprisingly, although the material's compressive strength of E20-CR0 (21.5 MPa) was much lower than M40 (45.1 MPa), the load capacity of the pipe repaired by E20-CR0 (14.8 kN) was higher than that by M40 (11.2 kN), as well as the sound concrete pipe (4.7 kN). The load capacity of the E40-CR30 pipe (27.9 kN) was 2.5 times M40 and 1.6 times M70, showing that the material strength is not the sole determining factor of pipe capacity. Tensile ductility also has a critical impact on structural capacity under the three-edge crushing test.

Apart from the enhancement of load capacity, the displacement capacity of the pipe under three-edge loading was also prominently improved. Once the external load reached the peak load, the load of Pipe_Ref, M40, and M70 dropped suddenly (Fig. 9(a)), while ECCs (Fig. 9(b)) hold residual capacity after peak load. The brittle failure mode of concrete-mortar pipe was transformed into ductile failure on concrete-ECC pipe composites. Fig. 11 shows the crack pattern of crushed pipes, where the mortar-concrete pipe broke into pieces with the mortar liner debonded from the original concrete pipe. In contrast, the ECC-concrete pipe maintained an oval shape after a displacement history that was more than 2 times of mortar-concrete pipe. Despite the presence of macro cracks in the host concrete, the ECC liner retain residual shape integrity and partial bonding to the concrete pipe (Fig. 11(b)). Owing to the ultra-high ductility and crack control ability, the macro crack from the host pipe was dispersed into multiple tiny cracks in the ECC lining so that the stress concentration and brittle failure were avoided. Consequently, the deform capacity of repaired pipe was significantly enhanced. Additionally, the residual load capacity of E40-CR30 after experiencing 20 mm of displacement was comparable to the peak value of the M70 pipe and larger than the M40 pipe (Fig. 9).

As the ECC-repaired pipe exhibited a distinct failure pattern from the mortar-repaired pipe (Fig. 11), E20-CR0 was selected for the leak-proof demonstration. Once the ECC-concrete pipe was loaded to the peak load, the pipe was unloaded and sealed on plywood (right part in Fig. 12). Although macro cracks exist in the concrete pipe and micro-cracks

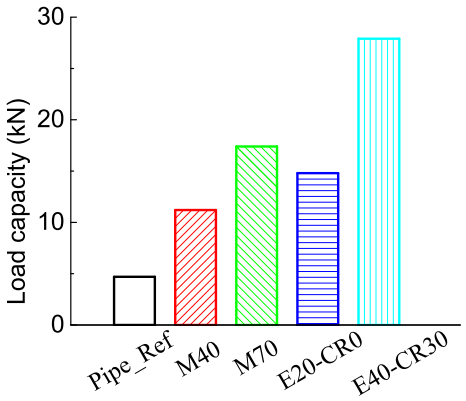

Fig. 10. The three-edge bearing load capacity of concrete pipe repaired with different materials.

(a) Mortar-repaired pipe (b) ECC-repaired pipe

Fig. 11. Failure pattern of the repaired concrete pipe after the three-edge loading test.

appeared in the ECC liner, no water leakage from the ECC-concrete pipe was detected after 24 h of water retainment, as revealed in Fig. 12.

This superior water tightness can be attributed to the rapid increase of fracture resistance of ECC. For cracks initiated from the inner surface (top and bottom zone in Fig. 12), the rapidly increased fracture resistance contributed by bridging fibers impeded crack propagation. Once the fracture resistance reached equilibrium with external driven force, the cracks were arrested and new cracks were initiated at other weak locations. As shown in Fig. 12, the cracks were trapped before reaching the pipe surfaces. Thus, the ECC pipe maintained structural integrity and water retention ability even after experiencing deformation beyond the peak load. For those cracks initiated from the concrete-ECC interface (left and right part in Fig. 12), the same phenomenon was also observed. The ECC repaired pipe retained residual structural capacity and maintained an intrinsic leak-proof function by preventing the macro crack from penetrating the full ECC liner.

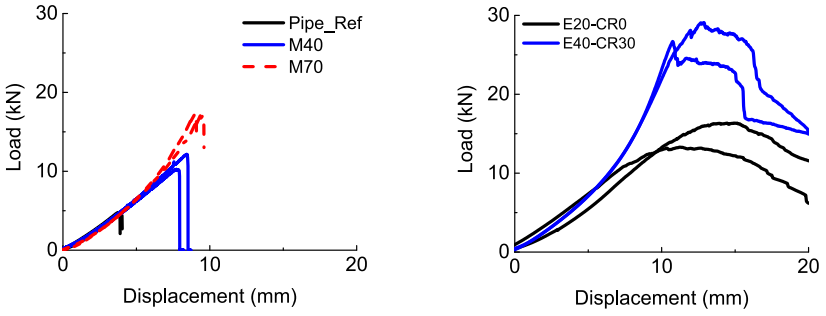

(a) Pipe_Ref and repaired with M40/M70 (b) Repaired with ECC

Fig. 9. The three-edge bearing load–displacement curves of concrete pipe repaired by ECC and mortars.

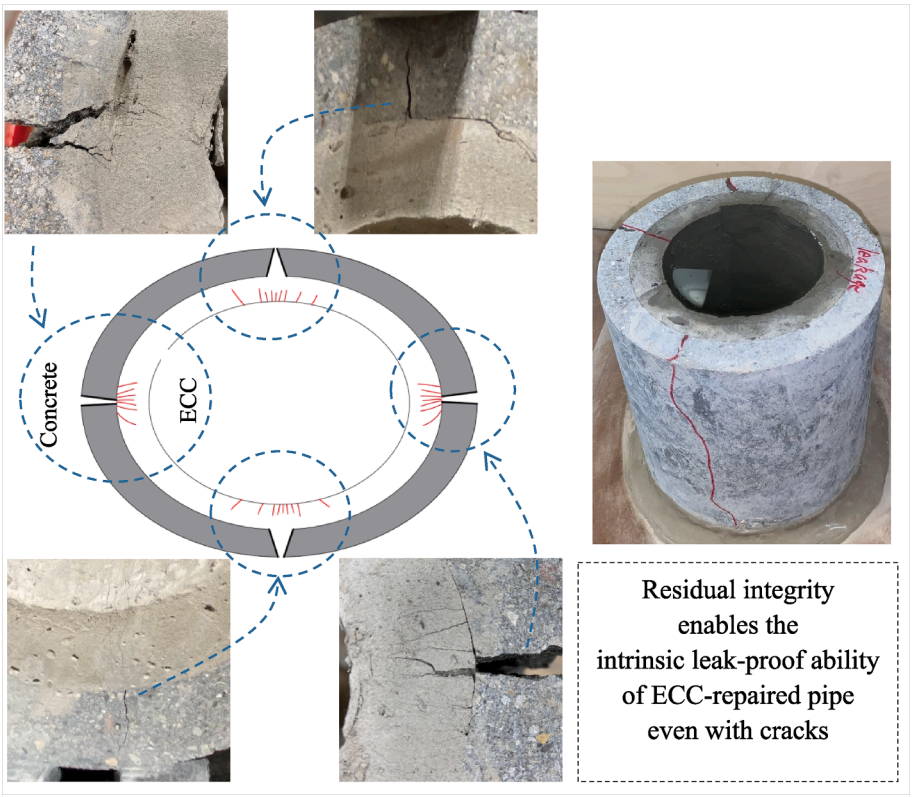

Fig. 12. Leak-proof demonstration of ECC repaired pipe.

Leakage is a precursor to structural failure. Once leakage occurs, the outflowing water washes out the soil around the pipe, resulting in poor bedding or ground settlement as well as pipe failure. Although sometimes cracks are inevitable due to aggressive environments and mechanical loads, the ECC repaired pipe can maintain water tightness due to its intrinsic leak-proof ability and low permeability (Section 3.2).

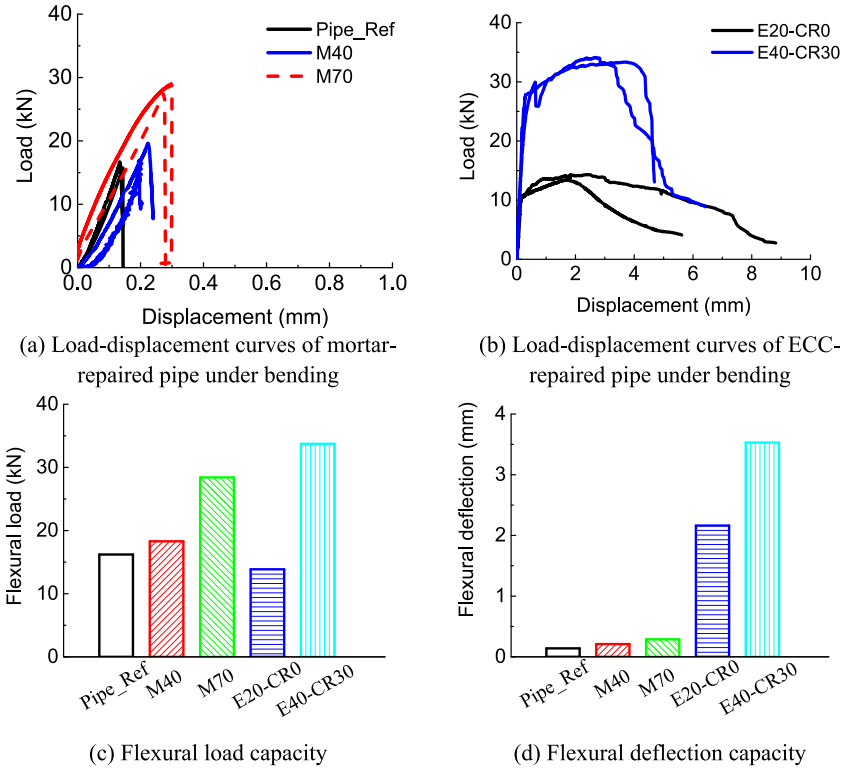

(a) Load-displacement curves of mortar-repaired pipe under bending

(b) Load-displacement curves of ECC-repaired pipe under bending

(c) Flexural load capacity

(d) Flexural deflection capacity

Fig. 13. Flexural load and displacement results of repaired pipes.

3.4. Retrofit performance under bending

Similar to the three-edge loading tests, mortar-repaired pipes showed a brittle failure pattern (Fig. 13(a)), while ECC-repaired pipes presented ductile failure under flexural load (Fig. 13(b)). After repair, the flexural load capacity of the M40 pipe (18.3 kN) was higher than the Pipe_Ref (16.2 kN), and M70 further increased the flexural load capacity of repaired pipe to 18.4 kN (Fig. 13(c)), consistent with the common perception that higher compressive strength of mortar results in a higher flexural capacity of the repaired pipe.

Different from the three-edge loading results, E20-CR0 obtained 13.9 kN of flexural load capacity, which is inferior to the Pipe_Ref due to the lower compressive and tensile strength of E20-CR0. The flexural load capacity of E40-CR30 was significantly enhanced to 33.7 kN, which was twice that of the original Pipe_Ref. The high tensile strength, ductility, and moderate compressive of E40-CR30 contributed to this enhancement.

Apart from the load capacity, the deflection capacity was insignificantly improved by M40 and M70 compared to Pipe_Ref. However, ECC notably upgraded the concrete pipe's deflection capacity. 15 and 25 times flexural deflection capacity was increased by E20-CR0 and E40-CR30, respectively. The improvement of deflection capacity benefited from the multiple crack ability and ultra-high ductility of ECC. As shown in Fig. 14, one major crack was observed for the concrete pipe repaired by mortar, while multiple tiny cracks were generated in the ECC liner. The considerable improvement of deflection capacity enables a safer repaired pipe under externally imposed deformation, such as poor bedding and ground settlement.

As demonstrated in Section 3.2–3.4, both the load and deformation capacity of the concrete were enhanced when repaired with ECC, even though the strength grade of E0-CR0 was low. Moreover, a leak-proof function of cracked pipe was obtained by ECC, attesting that ECC can structurally and functionally retrofit the concrete pipe.

For a given rehabilitated performance, a thinner liner is needed when ECC is used, especially E40-CR30 which is superior to M70. The reduced thickness leads to the ECC being a potentially lower cost and greener material than the conventional high-performance mortar as a pipe-repair material. Additionally, the reduced thickness of the ECC liner will maintain the water flow capacity to a maximum extent.

CIPP and sprayed cementitious materials are two widely used trenchless methods for pipe rehabilitation. CIPP has the advantages of high construction efficiency, maintained/enhanced hydraulic capacity, and chemical resistance. However, high cost, host pipe requirement (round shape, minor deterioration), and defects caused by installation and curing limit those advantages. The strict quality assurance, quality control, and long-term performance of CIPP require closer examination. Sprayed cementitious materials have low cost and high stiffness advantages. Nevertheless, the brittle material nature limits it mainly for non-structural applications, such as anti-leakage and anti-corrosion purposes.

While this study focuses on the material development for pipe structural retrofit, a centrifugally sprayed ECC technology has been developed by authors [12], aiming at applying the ECC as an inner repaired liner without open-dig activities, also called trenchless repair technology. The centrifugally sprayed ECC has been demonstrated with a no-dig requirement, fast construction, and wide application ranges. For example, varied diameters (0.3–5.0 m), changed pipe section/shape (round, oval, with unstraight turn) long length (up to 2700 m). Owing to the above merits, the durable LC3 ECC shows low-cost low carbon advantages at both the initial stage and full life cycle over other pipe repair methods, especially compared to replacing existing pipes. More discussions on applying ECC as a pipe repair material and its benefits can be found in the authors' previous study [1].

4. Conclusions

In this study, limestone calcined clay cement (LC3) was used in the greener ECC compared to the conventional Portland ECC. Two versions of ductile ECC with compressive strength of 21.5 MPa (E20-CR0) and 38.7 MPa (E40-CR30) were developed. Mortars with 45.1 MPa (M40) and 68.6 MPa (M70) compressive strength served as reference compositions. Finally, both ECC and mortars were utilized for pipe repair. Based on the experimental results at the material level (uniaxial tension and permeability test) and structural level (three-edge pipe loading, pipe leak-proof, and pipe bending tests), the following conclusions can be drawn:

1. All ECCs showed ultra-high tensile ductility over 5.4%. While crumb rubber reduced the compressive and tensile strength, the tensile ductility was considerably increased from 5.5% (E40-CR0 without crumb rubber) to 9.3% (E40-CR30 with 30 kg/m^3 of crumb rubber incorporation). In addition, the crack width of E40-CR30 was reduced to below 62 μm at 8% tensile strain.
2. The coefficient of permeability (*CoP*) of the developed LC3 ECC decreased with time evolution and showed comparable magnitude to the conventional ECC, suggesting a sufficient self-healing capacity to seal the cracks. The *CoP* of pre-cracked ECC dropped from 10^{-8} m/s at 28 d to 10^{-10} m/s at 42 d. The *CoP* of E40-CR30 ($5.77 * 10^{-10}$ m/s) was about one-third of E40-CR0 due to the tiny crack width of E40-CR30, suggesting a water-tight liner for pipe repair.
3. Under the three-edge loading test, the repaired pipes with lower-strength ECC lining attained higher load and deformation capacity than that those with higher-strength mortars. Specifically, the load capacity of the repaired pipe by E20-CR0 was 1.3 times that of M40, and E40-CR30 obtained 2.5 times that of M40 and 1.6 times that of M70. Both the strength and tensile ductility of the repair material are determining factors of the repaired pipe capacity.
4. Distinct from the brittle failure of mortar-repaired pipe, ECC distributed the macro crack into multiple tiny cracks, exhibiting an oval shape after loading. Owing to the ultra-high ductility and crack control ability, the cracked ECC pipe retained the structural integrity, enabling a residual loading capacity and intrinsic leak-proof function of cracked ECC pipe.

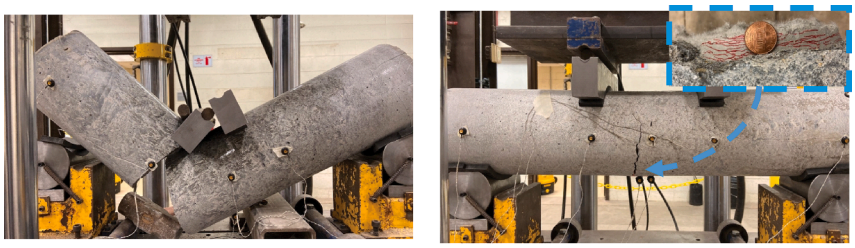

(a) Mortar-repaired pipe (b) ECC-repaired pipe

Fig. 14. Flexural failure pattern of the repaired concrete pipes.

5. The flexural load–displacement curve is similar to that of the three-edge loading test, i.e., ECC pipe presented ductile failure while mortar pipes showed brittle failure. Benefiting from the multiple crack ability and ultra-high ductility of ECC, the deflection capacity was upgraded 15 and 25 times by E20-CR0 and E40-CR30 compared to the original concrete pipe.

ECC has demonstrated the ability to structurally and functionally (leak-proof) retrofit the concrete pipe. A reduced-thickness of ECC liner can attain the same or even better-rehabilitated performance than the mortar liner with a larger thickness. Less material need suggests lower cost and carbon footprint, while maintaining high lining performance. While this lab-scale study demonstrates the benefits of LC3-ECC liner, further study of the retrofit effect of concrete pipes with larger diameters that meet practical applications is warranted.

CRediT authorship contribution statement

He Zhu: Conceptualization, Methodology, Investigation, Formal analysis, Writing – original draft, Writing – review & editing. **Tianyu Wang:** Investigation. **Yichao Wang:** Investigation. **Wei-Hsiu Hu:** Investigation. **Victor C. Li:** Funding acquisition, Project administration, Conceptualization, Writing – review & editing.

Declaration of Competing Interest

The authors declare that they have no known competing financial interests or personal relationships that could have appeared to influence the work reported in this paper.

Data availability

Data will be made available on request.

Acknowledgments

The authors acknowledge the generous help from Steve Donajkowski. The authors are grateful for the materials supplied by BASF Chemicals Company (water reducer), Entech Inc. (crumb rubber), and Elkem (silica fume).

References

[1] Zhu H, Wang T, Wang Y, Li VC. Trenchless rehabilitation for concrete pipelines of water infrastructure: a review from the structural perspective. Cem Concr Compos 2021;123:104193. https://doi.org/10.1016/j.cemconcomp.2021.104193.
[2] Zaneldin E, Al Khatib O, Ahmed W. Investigating the use of no-dig technologies for underground utilities in developing countries. Innov Infrastruct Solut 2020;5:1–12. https://doi.org/10.1007/s41062-020-0265-5.
[3] ASCE. 2021 Infrastructure Report Card. 2021.
[4] Yahong Z, Sheng H, Baosong M, Cong Z, Xuefeng Y, Zhongsen T, et al. Experiment and evaluation model of liner design for renewal of deteriorated reinforced concrete pipes utilizing cured-in-place-pipe technology. Tunn Undergr Sp Technol 2023;132:104866. https://doi.org/10.1016/J.TUST.2022.104866.
[5] Nuruddin M, DeCocker K, Sendesi SMT, Whelton AJ, Youngblood JP, Howarter JA. Influence of aggressive environmental aging on mechanical and thermo-mechanical properties of Ultra Violet (UV) Cured in Place Pipe liners. J Compos Mater 2020;54:3365–79. https://doi.org/10.1177/0021998320913988.
[6] Donaldson B, Whelton A. Impact of stormwater pipe lining materials on water quality. Transp Res Rec 2013:49–56. https://doi.org/10.3141/2362-07.
[7] American Water Works Association. Manual of Water Supply Practices: Rehabilitation of Water Mains (M28). Third. Denver; 2014.
[8] Li B, Zhu L, Fu X. Influence of grout strength and residual deformation on performance of rehabilitated RC Pipes. J Pipeline Syst Eng Pract 2020;11: 04020003. https://doi.org/10.1061/(asce)ps.1949-1204.0000448.
[9] Li BJ, Zhu LS, Li Y, Fu XS. Experimental investigation of an existing RCP rehabilitated with a grouted corrugated steel pipe. Math Probl Eng 2019;2019. doi: 10.1155/2019/7676359.
[10] Montes C, Allouche EN. Evaluation of the potential of geopolymer mortar in the rehabilitation of buried infrastructure. Struct Infrastruct Eng 2012;8:89–98. https://doi.org/10.1080/15732470903329314.
[11] Davidson JS, Kang J, Grimes TC, County S, Farrell J, Vaidya UK, et al. PVA Fiber reinforced shotcrete for rehabilitation and preventative maintenance of aging culverts. 2008.
[12] Zhu H, Zhang D, Li VC. Centrifugally sprayed engineered cementitious composites: rheology, mechanics, and structural retrofit for concrete pipes. Cem Concr Compos 2022;129:104473. https://doi.org/10.1016/j.cemconcomp.2022.104473.
[13] Li VC. Engineered Cementitious Composites (ECC). Springer; 2019. doi: 10.1007/978-3-662-58438-5.
[14] Zhu H, Zhang D, Wang T, Wu H, Li VC. Mechanical and self-healing behavior of low carbon engineered cementitious composites reinforced with PP-fibers. Constr Build Mater 2020;259:119805. https://doi.org/10.1016/j.conbuildmat.2020.119805.
[15] Yu K, Zhu H, Hou M, Li VC. Self-healing of PE-fiber reinforced lightweight high-strength engineered cementitious composite. Cem Concr Compos 2021;123: 104209. https://doi.org/10.1016/j.cemconcomp.2021.104209.
[16] Lepech MD, Li VC. Water permeability of engineered cementitious composites. Cem Concr Compos 2009;31:744–53. https://doi.org/10.1016/j.cemconcomp.2009.07.002.
[17] Zhang Z, Zhang Q. Self-healing ability of Engineered Cementitious Composites (ECC) under different exposure environments. Constr Build Mater 2017;156: 142–51. https://doi.org/10.1016/J.CONBUILDMAT.2017.08.166.
[18] Li VC, Herbert E. Robust self-healing concrete for sustainable infrastructure. J Adv Concr Technol 2012;10:207–18.
[19] Ohno M, Li VC. Sulfuric acid resistance of strain hardening fibre reinforced geopolymer composite. Indian Concr J 2019;93:47–53.
[20] Wang T, Zhang D, Zhu H, Ma B, Li VC. Durability and self-healing of engineered cementitious composites exposed to simulated sewage environments. Cem Concr Compos 2022;129:104500. https://doi.org/10.1016/j.cemconcomp.2022.104500.
[21] Shoji D, Zhu H, Zhang D, Li VC. The greening of engineered cementitious composites (ECC): a review. Constr Build Mater 2022;327:126701. https://doi.org/10.1016/j.conbuildmat.2022.126701.
[22] Lepech MD, Li VC, Robertson RE, Keoleian GA. Design of green engineered cementitious composites for improved sustainability. ACI Mater J 2008;105: 567–75. https://doi.org/10.14359/20198.
[23] Zhu H, Zhang D, Wang Y, Wang T, Li VC. Development of self-stressing Engineered Cementitious Composites (ECC). Cem Concr Compos 2021;118:103936. doi: 10.1016/j.cemconcomp.2021.103936.
[24] Huang X, Ranade R, Ni W, Li VC. Development of green engineered cementitious composites using iron ore tailings as aggregates. Constr Build Mater 2013;44: 757–64. https://doi.org/10.1016/j.conbuildmat.2013.03.088.
[25] Zhang Z, Yang F, Liu JC, Wang S. Eco-friendly high strength, high ductility engineered cementitious composites (ECC) with substitution of fly ash by rice husk ash. Cem Concr Res 2020;137:106200. https://doi.org/10.1016/j.cemconres.2020.106200.
[26] Yu KQ, Zhu WJ, Ding Y, Lu ZD, Yu J tao, Xiao JZ. Micro-structural and mechanical properties of ultra-high performance engineered cementitious composites (UHP-ECC) incorporation of recycled fine powder (RFP). Cem Concr Res 2019;124: 105813. doi: 10.1016/j.cemconres.2019.105813.
[27] Borg RP, Cuenca E, Garofalo R, Schillani F, Nasner ML, Ferrara L. Performance assessment of ultra-high durability concrete produced from recycled ultra-high durability concrete. Front Built Environ 2021;7:1–20. https://doi.org/10.3389/fbuil.2021.648220.
[28] Scrivener K, Martirena F, Bishnoi S, Maity S. Calcined clay limestone cements (LC3). Cem Concr Res 2018;114:49–56. doi: 10.1016/j.cemconres.2017.08.017.
[29] Zhang D, Jaworska B, Zhu H, Dahlquist K, Li VC. Engineered Cementitious Composites (ECC) with limestone calcined clay cement (LC3). Cem Concr Compos 2020;114:103766. https://doi.org/10.1016/j.cemconcomp.2020.103766.
[30] Hou M, Zhang D, Li VC. Material processing, microstructure, and composite properties of low carbon Engineered Cementitious Composites (ECC). Cem Concr Compos 2022;134:104790. https://doi.org/10.1016/J.CEMCONCOMP.2022.104790.
[31] Zhu H, Yu K, McGee W, Ng TY, Li VC. Limestone calcined clay cement for three-dimensional-printed engineered cementitious composites. ACI Mater J 2021;118: 111–22. https://doi.org/10.14359/51733109.
[32] Zhu H, Yu K, Li VC. Citric acid influence on sprayable CSA-ECC fresh / hardened properties. ACI Mater J 2021;118:39–48. https://doi.org/10.14359/51733103.
[33] Zhu H, Yu K, Li VC. Sprayable engineered cementitious composites (ECC) using calcined clay limestone cement (LC3) and PP fiber. Cem Concr Compos 2021;115: 103868. doi: 10.1016/j.cemconcomp.2020.103868.
[34] Huang BT, Li QH, Xu SL, Zhou B. Strengthening of reinforced concrete structure using sprayable fiber-reinforced cementitious composites with high ductility. Compos Struct 2019;220:940–52. https://doi.org/10.1016/J.COMPSTRUCT.2019.04.061.
[35] Billington SL, Kyriakides MA, Blackard B, Willam K, Stavridis A, Shing PB. Evaluation of a sprayable, ductile cement-based composite for the seismic retrofit of unreinforced masonry infills. In: Improv Seism Perform Exist Build Other Struct - Proc 2009 ATC SEI Conf Improv Seism Perform Exist Build Other Struct 2009; 41084:823–34. doi: 10.1061/41084(364)75.
[36] ASTM C1437-15. Standard test method for flow of hydraulic cement mortar. West Conshohocken, PA: ASTM International; 2015. Available from: www.astm.org n.d.
[37] ASTM C497M-19. Standard test methods for concrete pipe, concrete box sections, manhole sections, or tile (metric). West Conshohocken, PA: ASTM International; 2019. Available from: www.astm.org n.d. doi: 10.1520/C0497M-19.
[38] Tsivilis S, Tsantilas J, Kakali G, Chaniotakis E, Sakellariou A. The permeability of Portland limestone cement concrete. Cem Concr Res 2003;33:1465–71. https://doi.org/10.1016/S0008-8846(03)00092-9.

[39] Banthia N, Biparva A, Mindess S. Permeability of concrete under stress. Cem Concr Res 2005;35:1651–5. https://doi.org/10.1016/J.CEMCONRES.2004.10.044.
[40] Hoseini M, Bindiganavile V, Banthia N. The effect of mechanical stress on permeability of concrete: a review. Cem Concr Compos 2009;31:213–20. https://doi.org/10.1016/J.CEMCONCOMP.2009.02.003.
[41] Li VC, Yang E-H. Self healing in concrete materials. Self Heal. Mater. Springer; 2007. p. 161–93.
[42] Liu H, Zhang Q, Gu C, Su H, Li V. Influence of microcrack self-healing behavior on the permeability of Engineered Cementitious Composites. Cem Concr Compos 2017;82:14–22. https://doi.org/10.1016/j.cemconcomp.2017.04.004.
[43] Liu H, Zhang Q, Gu C, Su H, Li VC. Influence of micro-cracking on the permeability of engineered cementitious composites. Cem Concr Compos 2016;72:104–13. https://doi.org/10.1016/j.cemconcomp.2016.05.016.